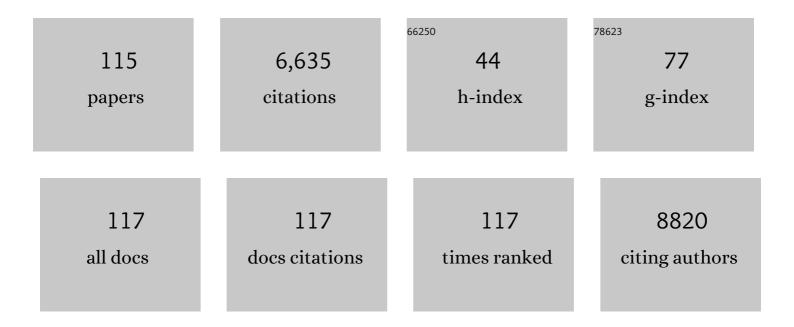
List of Publications by Year in descending order

Source: https://exaly.com/author-pdf/7486836/publications.pdf Version: 2024-02-01



Υινσητι Ιανις

#	Article	IF	CITATIONS
1	A Unique Structural Highly Compacted Binderâ€Free Siliconâ€Based Anode with High Electronic Conductivity for Highâ€Performance Lithiumâ€lon Batteries. Small Structures, 2022, 3, 2100174.	6.9	22
2	A Redox Couple Strategy Enables Longâ€Cycling Li―and Mnâ€Rich Layered Oxide Cathodes by Suppressing Oxygen Release. Advanced Materials, 2022, 34, e2108543.	11.1	24
3	New Insights into the Effects of Zr Substitution and Carbon Additive on Li <sub>3–<i>x</i></sub> Er <sub>1–<i>x</i></sub> Zr <sub><i>x</i></sub> Cl <sub>6</sub> Halide Solid Electrolytes. ACS Applied Materials & Interfaces, 2022, 14, 8095-8105.	4.0	36
4	Hybrid Design of Bulkâ€Na Metal Anode to Minimize Cycleâ€Induced Interface Deterioration of Solid Na Metal Battery. Advanced Energy Materials, 2022, 12, .	10.2	25
5	From fundamentals and theories to heterostructured electrocatalyst design: An in-depth understanding of alkaline hydrogen evolution reaction. Nano Energy, 2022, 98, 107231.	8.2	76
6	Ion Hopping: Design Principles for Strategies to Improve Ionic Conductivity for Inorganic Solid Electrolytes. Small, 2022, 18, e2107064.	5.2	23
7	Toward enhanced alkaline hydrogen electrocatalysis with transition metal-functionalized nitrogen-doped carbon supports. Chinese Journal of Catalysis, 2022, 43, 1351-1359.	6.9	6
8	Cobalt Single Atoms Enabling Efficient Methanol Oxidation Reaction on Platinum Anchored on Nitrogenâ€Doped Carbon. Small, 2022, 18, e2107067.	5.2	23
9	A robust, highly reversible, mixed conducting sodium metal anode. Science Bulletin, 2021, 66, 179-186.	4.3	29
10	Interface engineering of heterostructured electrocatalysts towards efficient alkaline hydrogen electrocatalysis. Science Bulletin, 2021, 66, 85-96.	4.3	127
11	Recent progress on hybrid electrocatalysts for efficient electrochemical CO2 reduction. Nano Energy, 2021, 80, 105504.	8.2	78
12	Interface Engineering of Air Electrocatalysts for Rechargeable Zinc–Air Batteries. Advanced Energy Materials, 2021, 11, 2002762.	10.2	129
13	Konjac glucomannan biopolymer as a multifunctional binder to build a solid permeable interface on Na <sub>3</sub> V <sub>2</sub> (PO <sub>4</sub> ) <sub>3</sub> /C cathodes for high-performance sodium ion batteries. Journal of Materials Chemistry A, 2021, 9, 9864-9874.	5.2	16
14	A Novel Perovskite Electron–Ion Conductive Coating to Simultaneously Enhance Cycling Stability and Rate Capability of Li <sub>1.2</sub> Ni <sub>0.13</sub> Co <sub>0.13</sub> Mn <sub>0.54</sub> O <sub>2</sub> Cathode Material for Lithiumâ€ion Batteries. Small, 2021, 17, e2008132.	5.2	28
15	Porous Bilayer Electrodeâ€Guided Gas Diffusion for Enhanced CO <sub>2</sub> Electrochemical Reduction. Advanced Energy and Sustainability Research, 2021, 2, 2100083.	2.8	10
16	2D Metalâ€Free Nanomaterials Beyond Graphene and Its Analogues toward Electrocatalysis Applications. Advanced Energy Materials, 2021, 11, 2101202.	10.2	24
17	Atomic-Level Modulation of the Interface Chemistry of Platinum–Nickel Oxide toward Enhanced Hydrogen Electrocatalysis Kinetics. Nano Letters, 2021, 21, 4845-4852.	4.5	31
18	Manipulating the Coordination Chemistry of RuN(O)C Moieties for Fast Alkaline Hydrogen Evolution Kinetics. Advanced Functional Materials, 2021, 31, 2100698.	7.8	74

#	Article	IF	CITATIONS
19	Conversionâ€Alloying Anode Materials for Sodium Ion Batteries. Small, 2021, 17, e2101137.	5.2	102
20	Singleâ€Atom Electrocatalysts for Multiâ€Electron Reduction of CO <sub>2</sub> . Small, 2021, 17, e2101443.	5.2	44
21	Amino Acidâ€Induced Interface Charge Engineering Enables Highly Reversible Zn Anode. Advanced Functional Materials, 2021, 31, 2103514.	7.8	156
22	Reversible Magnesium Metal Anode Enabled by Cooperative Solvation/Surface Engineering in Carbonate Electrolytes. Nano-Micro Letters, 2021, 13, 195.	14.4	24
23	Latticeâ€Confined Ir Clusters on Pd Nanosheets with Charge Redistribution for the Hydrogen Oxidation Reaction under Alkaline Conditions. Advanced Materials, 2021, 33, e2105400.	11.1	76
24	A Novel Tin-Bonded Silicon Anode for Lithium-Ion Batteries. ACS Applied Materials & Interfaces, 2021, 13, 45578-45588.	4.0	25
25	Manganese hexacyanoferrate reinforced by PEDOT coating towards high-rate and long-life sodium-ion battery cathode. Journal of Materials Chemistry A, 2020, 8, 3222-3227.	5.2	73
26	A Ga–Sn liquid metal-mediated structural cathode for Li–O2 batteries. Materials Today Energy, 2020, 18, 100559.	2.5	3
27	Hexagonal Boron Nitride as a Multifunctional Support for Engineering Efficient Electrocatalysts toward the Oxygen Reduction Reaction. Nano Letters, 2020, 20, 6807-6814.	4.5	82
28	Low oordinate Iridium Oxide Confined on Graphitic Carbon Nitride for Highly Efficient Oxygen Evolution. Angewandte Chemie, 2019, 131, 12670-12674.	1.6	15
29	Low oordinate Iridium Oxide Confined on Graphitic Carbon Nitride for Highly Efficient Oxygen Evolution. Angewandte Chemie - International Edition, 2019, 58, 12540-12544.	7.2	208
30	Enabling Full Conversion Reaction with High Reversibility to Approach Theoretical Capacity for Sodium Storage. Advanced Functional Materials, 2019, 29, 1906680.	7.8	29
31	An Allâ€Prussianâ€Blueâ€Based Aqueous Sodiumâ€ion Battery. ChemElectroChem, 2019, 6, 4848-4853.	1.7	44
32	A Universal Strategy to Fabricate Metal Sulfides@Carbon Fibers As Freestanding and Flexible Anodes for High-Performance Lithium/Sodium Storage. ACS Applied Energy Materials, 2019, 2, 4421-4427.	2.5	17
33	Si/Ti3SiC2 composite anode with enhanced elastic modulus and high electronic conductivity for lithium-ion batteries. Journal of Power Sources, 2019, 431, 55-62.	4.0	32
34	Na <sub>2</sub> Fe(SO <sub>4</sub> ) <sub>2</sub> : an anhydrous 3.6ÂV, low-cost and good-safety cathode for a rechargeable sodium-ion battery. Journal of Materials Chemistry A, 2019, 7, 13197-13204.	5.2	32
35	Intercalation Pseudocapacitance Boosting Ultrafast Sodium Storage in Prussian Blue Analogs. ChemSusChem, 2019, 12, 2415-2420.	3.6	28
36	Hetero-interface constructs ion reservoir to enhance conversion reaction kinetics for sodium/lithium storage. Energy Storage Materials, 2019, 18, 107-113.	9.5	105

#	Article	IF	CITATIONS
37	Prussian Blue Analogs for Rechargeable Batteries. IScience, 2018, 3, 110-133.	1.9	327
38	Gradient substitution: an intrinsic strategy towards high performance sodium storage in Prussian blue-based cathodes. Journal of Materials Chemistry A, 2018, 6, 8947-8954.	5.2	55
39	A novel strategy to significantly enhance the initial voltage and suppress voltage fading of a Li- and Mn-rich layered oxide cathode material for lithium-ion batteries. Journal of Materials Chemistry A, 2018, 6, 3610-3624.	5.2	78
40	Synthesis of hierarchical porous carbon from metal carbonates towards high-performance lithium storage. Green Chemistry, 2018, 20, 1484-1490.	4.6	32
41	SiO2 nanoparticles enhanced silicone resin as the matrix for Fe soft magnetic composites with improved magnetic, mechanical and thermal properties. Journal of Alloys and Compounds, 2018, 741, 35-43.	2.8	51
42	Hierarchical Structures: Spatially Configuring Wrinkle Pattern and Multiscale Surface Evolution with Structural Confinement (Adv. Funct. Mater. 1/2018). Advanced Functional Materials, 2018, 28, 1870005.	7.8	0
43	Engineering capacitive contribution in nitrogen-doped carbon nanofiber films enabling high performance sodium storage. Carbon, 2018, 130, 145-152.	5.4	58
44	Bubble-supported engineering of hierarchical CuCo <sub>2</sub> S <sub>4</sub> hollow spheres for enhanced electrochemical performance. Journal of Materials Chemistry A, 2018, 6, 5265-5270.	5.2	103
45	Spatially Configuring Wrinkle Pattern and Multiscale Surface Evolution with Structural Confinement. Advanced Functional Materials, 2018, 28, 1704228.	7.8	28
46	Readily Exfoliated TiSe <sub>2</sub> Nanosheets for Highâ€Performance Sodium Storage. Chemistry - A European Journal, 2018, 24, 1193-1197.	1.7	40
47	Li- and Mn-rich layered oxide cathode materials for lithium-ion batteries: a review from fundamentals to research progress and applications. Molecular Systems Design and Engineering, 2018, 3, 748-803.	1.7	127
48	Investigations on molybdenum dinitride as a promising anode material for Na-ion batteries from first-principle calculations. Journal of Alloys and Compounds, 2017, 701, 875-881.	2.8	17
49	Ultrafast, Highly Reversible, and Cycleâ€6table Lithium Storage Boosted by Pseudocapacitance in Snâ€Based Alloying Anodes. Advanced Materials, 2017, 29, 1606499.	11.1	102
50	Pseudocapacitance-Enhanced Li-Ion Microbatteries Derived by a TiN@TiO2 Nanowire Anode. CheM, 2017, 2, 404-416.	5.8	90
51	SnS <sub>2</sub> Nanowall Arrays toward High-Performance Sodium Storage. ACS Applied Materials & Interfaces, 2017, 9, 6979-6987.	4.0	83
52	A High Capacity, Good Safety and Low Cost Na <sub>2</sub> FeSiO <sub>4</sub> -Based Cathode for Rechargeable Sodium-Ion Battery. ACS Applied Materials & Interfaces, 2017, 9, 22369-22377.	4.0	52
53	Pseudocapacitanceâ€Enhanced Highâ€Rate Lithium Storage in "Honeycombâ€â€like Mn <sub>2</sub> O <sub>3</sub> Anodes. ChemElectroChem, 2017, 4, 565-569.	1.7	19
54	Engineering Hierarchical Hollow Nickel Sulfide Spheres for Highâ€Performance Sodium Storage. Advanced Functional Materials, 2016, 26, 7479-7485.	7.8	174

#	Article	IF	CITATIONS
55	Twoâ€Dimensional Cobalt…Nickelâ€Based Oxide Nanosheets for Highâ€Performance Sodium and Lithium Storage. Chemistry - A European Journal, 2016, 22, 18060-18065.	1.7	28
56	Multiple unpinned Dirac points in group-Va single-layers with phosphorene structure. Npj Computational Materials, 2016, 2, .	3.5	57
57	Everâ€Increasing Pseudocapacitance in RGO–MnO–RGO Sandwich Nanostructures for Ultrahighâ€Rate Lithium Storage. Advanced Functional Materials, 2016, 26, 2198-2206.	7.8	238
58	Prussian Blue@C Composite as an Ultrahighâ€Rate and Longâ€Life Sodiumâ€Ion Battery Cathode. Advanced Functional Materials, 2016, 26, 5315-5321.	7.8	328
59	Titanium dioxide nanotrees for high-capacity lithium-ion microbatteries. Journal of Materials Chemistry A, 2016, 4, 10593-10600.	5.2	46
60	Bismuth sulfide: A high-capacity anode for sodium-ion batteries. Journal of Power Sources, 2016, 309, 135-140.	4.0	122
61	Enhanced electrocatalytic performance of Co3O4/Ketjen-black cathodes for Li–O2 batteries. Journal of Alloys and Compounds, 2015, 653, 604-610.	2.8	13
62	Evolution of phosphate coatings during high-temperature annealing and its influence on the Fe and FeSiAl soft magnetic composites. Journal of Alloys and Compounds, 2015, 644, 124-130.	2.8	102
63	Rational design of metal oxide nanocomposite anodes for advanced lithium ion batteries. Journal of Power Sources, 2015, 282, 1-8.	4.0	38
64	In situ growth of FeS microsheet networks with enhanced electrochemical performance for lithium-ion batteries. Journal of Materials Chemistry A, 2015, 3, 8742-8749.	5.2	86
65	Anatase TiO2 ultrathin nanobelts derived from room-temperature-synthesized titanates for fast and safe lithium storage. Scientific Reports, 2015, 5, 11804.	1.6	75
66	Spatially-confined lithiation–delithiation in highly dense nanocomposite anodes towards advanced lithium-ion batteries. Energy and Environmental Science, 2015, 8, 1471-1479.	15.6	69
67	Enhanced Reaction Kinetics and Structure Integrity of Ni/SnO <sub>2</sub> Nanocluster toward High-Performance Lithium Storage. ACS Applied Materials & Interfaces, 2015, 7, 26367-26373.	4.0	35
68	A promising cathode material of sodium iron–nickel hexacyanoferrate for sodium ion batteries. Journal of Power Sources, 2015, 275, 45-49.	4.0	137
69	Scalable synthesis of Fe3O4/C composites with enhanced electrochemical performance as anode materials for lithium-ion batteries. Journal of Alloys and Compounds, 2014, 582, 563-568.	2.8	31
70	High rate Li4Ti5O12–Fe2O3 and Li4Ti5O12–CuO composite anodes for advanced lithium ion batteries. Journal of Alloys and Compounds, 2014, 603, 202-206.	2.8	30
71	Amorphous Fe2O3 as a high-capacity, high-rate and long-life anode material for lithium ion batteries. Nano Energy, 2014, 4, 23-30.	8.2	307
72	Reversible Conversion-Alloying of Sb <sub>2</sub> O <sub>3</sub> as a High-Capacity, High-Rate, and Durable Anode for Sodium Ion Batteries. ACS Applied Materials & Interfaces, 2014, 6, 19449-19455.	4.0	143

#	Article	IF	CITATIONS
73	Fe <sub>2</sub> O <sub>3</sub> –Ag Porous Film Anodes for Ultrahighâ€Rate Lithiumâ€lon Batteries. ChemElectroChem, 2014, 1, 1155-1160.	1.7	18
74	Room temperature ferromagnetism of amorphous MgO films prepared by pulsed laser deposition. Applied Physics A: Materials Science and Processing, 2014, 115, 997-1001.	1.1	18
75	Effect of processing parameters on the magnetic properties and microstructures of molybdenum permalloy compacts made by powder metallurgy. Journal of Alloys and Compounds, 2014, 594, 153-157.	2.8	34
76	Transition metal oxides for high performance sodium ion battery anodes. Nano Energy, 2014, 5, 60-66.	8.2	361
77	Enhanced lithium storage performance in three-dimensional porous SnO2-Fe2O3 composite anode films. Electrochimica Acta, 2014, 136, 27-32.	2.6	21
78	Origin of room temperature ferromagnetism in MgO films. Applied Physics Letters, 2013, 102, .	1.5	53
79	Phase-tailored synthesis of tin oxide–graphene nanocomposites for anodes and their enhanced lithium-ion battery performance. Materials Letters, 2013, 91, 16-19.	1.3	8
80	Structure and magnetic properties of γ′-Fe4N films grown on MgO-buffered Si (001). Physica B: Condensed Matter, 2012, 407, 4783-4786.	1.3	6
81	Anomalous Magnetization Behavior of Fe-N Films Deposited by Reactive Pulsed Laser Deposition. IEEE Transactions on Magnetics, 2012, 48, 2899-2902.	1.2	1
82	Defect-induced room temperature ferromagnetism in Fe and Na co-doped ZnO nanoparticles. Journal of Alloys and Compounds, 2012, 521, 90-94.	2.8	31
83	Electrostatic Spray Deposition of Porous SnO <sub>2</sub> /Graphene Anode Films and Their Enhanced Lithium-Storage Properties. ACS Applied Materials & Interfaces, 2012, 4, 6216-6220.	4.0	100
84	Abnormal behaviors in electrical transport properties of cobalt-doped tin oxide thin films. Journal of Materials Chemistry, 2012, 22, 16060.	6.7	22
85	Effect of defects on room-temperature ferromagnetism in Co and Na co-doped ZnO. Applied Physics A: Materials Science and Processing, 2012, 107, 919-923.	1.1	11
86	Fe65B22Nd9Mo4 bulk nanocomposite permanent magnets produced by crystallizing amorphous precursors. Journal of Magnetism and Magnetic Materials, 2012, 324, 1613-1616.	1.0	10
87	Unusual enhancement in electrical conductivity of tin oxide thin films with zinc doping. Physical Chemistry Chemical Physics, 2011, 13, 5760.	1.3	18
88	Evidence of the defect-induced ferromagnetism in Na and Co codoped ZnO. Applied Physics Letters, 2011, 98, 012502.	1.5	43
89	Application of nBu2Sn(acac)2 for the deposition of nanocrystallite SnO2 films: Nucleation, growth and physical properties. Journal of Alloys and Compounds, 2011, 509, 7798-7802.	2.8	6
90	Optimization of BaZr0.1Ce0.7Y0.2O3â^îî-based proton-conducting solid oxide fuel cells with a cobalt-free proton-blocking La0.7Sr0.3FeO3â^îr–Ce0.8Sm0.2O2â^îî composite cathode. International Journal of Hydrogen Energy, 2011, 36, 9956-9966.	3.8	38

#	Article	IF	CITATIONS
91	A stable NH4PO3-glass proton conductor for intermediate temperature fuel cells. Solid State Ionics, 2011, 192, 108-112.	1.3	9
92	A novel electronic current-blocked stable mixed ionic conductor for solid oxide fuel cells. Journal of Power Sources, 2011, 196, 62-68.	4.0	73
93	Low-temperature solid oxide fuel cells with novel La0.6Sr0.4Co0.8Cu0.2O3â^1̂ perovskite cathode and functional graded anode. Journal of Power Sources, 2010, 195, 1624-1629.	4.0	29
94	The growth of nanoscale ZnO films by pulsed-spray evaporation chemical vapor deposition and their structural, electric and optical properties. Thin Solid Films, 2010, 519, 284-288.	0.8	3
95	Effect of Nucleation and Growth Kinetics on the Electrical and Optical Properties of Undoped ZnO Films. Journal of Physical Chemistry C, 2010, 114, 5121-5125.	1.5	10
96	Investigation of Growth, Structural and Optical Properties of CeO <sub>2</sub> Nanocrystalline Thin Films Prepared by Pulsed Spray-Evaporation Chemical Vapor Deposition (PSE-CVD). Nanoscience and Nanotechnology Letters, 2009, 1, 134-139.	0.4	3
97	A high performance intermediate temperature fuel cell based on a thick oxide–carbonate electrolyte. Journal of Power Sources, 2009, 194, 967-971.	4.0	47
98	Synthesis, characterization, and kinetic study of Mn(DPM)3 used as precursor for MOCVD. Ionics, 2009, 15, 627-633.	1.2	0
99	A stable and easily sintering BaCeO3-based proton-conductive electrolyte. Journal of Alloys and Compounds, 2009, 473, 323-329.	2.8	53
100	Stability and conductivity study of NH4PO3–PTFE composites at intermediate temperatures. Journal of Alloys and Compounds, 2009, 480, 874-877.	2.8	9
101	Changes in the structural and optical properties of CeO2 nanocrystalline films: Effect of film thickness. Journal of Alloys and Compounds, 2009, 485, L52-L55.	2.8	32
102	Low-temperature protonic ceramic membrane fuel cells (PCMFCs) with SrCo0.9Sb0.1O3â~δ cubic perovskite cathode. Journal of Power Sources, 2008, 185, 937-940.	4.0	23
103	A simple and easy one-step fabrication of thin BaZr0.1Ce0.7Y0.2O3â^1^ electrolyte membrane for solid oxide fuel cells. Journal of Membrane Science, 2008, 325, 6-10.	4.1	29
104	Stable, easily sintered BaCe0.5Zr0.3Y0.16Zn0.04O3â^îr´ electrolyte-based protonic ceramic membrane fuel cells with Ba0.5Sr0.5Zn0.2Fe0.8O3â^îr´ perovskite cathode. Journal of Power Sources, 2008, 183, 479-484.	4.0	46
105	Electrostatic Spray Assembly of Nanostructured La[sub 0.7]Ca[sub 0.3]CrO[sub 3â~'Î] Films. Journal of the Electrochemical Society, 2007, 154, E107.	1.3	10
106	Synthesis and Characterization of Pr(DPM)3 Served as Precursor for MOCVD. Chemical Research in Chinese Universities, 2007, 23, 258-262.	1.3	0
107	Fabrication and characterization of Y2O3 stabilized ZrO2 films deposited with aerosol-assisted MOCVD. Solid State Ionics, 2007, 177, 3405-3410.	1.3	30
108	An ammonia fuelled SOFC with a BaCe0.9Nd0.1O3â~δ thin electrolyte prepared with a suspension spray. Journal of Power Sources, 2007, 170, 38-41.	4.0	112

#	Article	IF	CITATIONS
109	Synthesis of LaCrO3 films using spray pyrolysis technique. Materials Letters, 2007, 61, 1908-1911.	1.3	16
110	Decomposition Behavior of M(DPM)n (DPM = 2,2,6,6-Tetramethyl-3,5-heptanedionato; n = 2, 3, 4). Journal of Physical Chemistry A, 2006, 110, 13479-13486.	1.1	26
111	Deposition of Sm2O3 doped CeO2 thin films from Ce(DPM)4 and Sm(DPM)3 (DPM=2,2,6,6-tetramethyl-3,5-heptanedionato) by aerosol-assisted metal–organic chemical vapor deposition. Thin Solid Films, 2006, 510, 88-94.	0.8	13
112	Formation and Rate Processes of Y[sub 2]O[sub 3] Stabilized ZrO[sub 2] Thin Films from Zr(DPM)[sub 4] and Y(DPM)[sub 3] by Cold-Wall Aerosol-Assisted MOCVD. Journal of the Electrochemical Society, 2005, 152, C498.	1.3	12
113	Synthesis and characterization of Sm(DPM)3 used as precursor for MOCVD. Journal of Crystal Growth, 2004, 267, 256-262.	0.7	13
114	Synthesis and characterization of volatile metal β-diketonate chelates of M(DPM)n (M=Ce, Gd, Y, Zr,) Tj ETQq0	0 0 rgBT /(	Dverlock 10 Tf

115	Deposition of Y2O3 stabilized ZrO2 thin films from Zr(DPM)4 and Y(DPM)3 by aerosol-assisted MOCVD. Materials Letters, 2003, 57, 3833-3838.	1.3	14	
-----	---	-----	----	--